Texila International Journal of Public Health
ISSN: 2520-3134
DOI: 10.21522/TIJPH.2013.13.02.Art061

Cardiac Disease Detection and Classification System using Machine Learning (ML)

R. Radhika*, Rashima Mahajan
Computer Science and Engineering Department, Manav Rachna International Institute of Research and Studies, Faridabad, Haryana 121004.

Abstract

In cardiac diagnostics, the application of Magnetic Resonance Imaging (MRI)is crucial. The detection of cardiac structures and anomalies can be improved by the enhancing image contrast. Here, cardiac lesions like tumors, scars, and irregularities in the heart are effectively detected and analyzed by the application of Machine Learning (ML) algorithms. The normal and abnormal tissues can be effectively distinguished by utilizing the classifiers. Early detection (ED) and early treatment was also facilitated by this classifier. In Medical Image Processing (MIP), a novel method that integrates the hybrid optimizations inspired by cetacean behaviors with Sand Cat Swarm Optimization (SCSO), named COA-SCSO was presented in this study. To enhance cardiac MRI Image Qualities (IQ), techniques like Noise Reductions (NR) and Contrast Enhancements (CE) are utilized by these hybrid optimizations, and enhancing cardiac MRI IQ is the objective of these hybrid optimizations. To classify the cardiac conditions using CMRI (Cardiac- MRI) data, the Proximal Support Vector Machine with Generalized Eigenvalue (PSVM-GE) improved by Particle Swarm Optimization (PSO) are used. The benefits of GE- based classifications are used, and it may support the suggested method in detecting patterns from improved cardiac MRI images. For accurate and effective detections of heart conditions, this suggested approach serves as a basis framework. Multidisciplinary approaches may result from the integration of ML methods with optimizations, and it will enhance Medical IQ. Contrast Enhancement (CE), NR, are facilitated by the suggested COA-SCSO model, and this model also enhances classification performance. The reliable and accurate cardiac anomalies detection was ensured by this suggested model. The Clinical Decision-Making (CDM) in cardiology was then improved by the study, and it was demonstrated by the outcomes. This will contribute an effective Computer-Aided Diagnostic (CAD) systems.

Keywords: *Classification and Cardiac Diseases, Contrast-Enhanced Cardiac MRI (CE-CMRI), Hybrid Optimization Algorithm (HOA), Particle Swarm Optimization (PSO), Proximal Support Vector Machine (PSVM) with Generalized Eigenvalue (GE).*

Introduction

Globally, Cardiovascular diseases (CVD) are one of the most prevalent cause of morbidity and mortality, so advanced diagnostic technique is needed. Because these advanced diagnostic methods assist in ED and early treatment [1]. The high-resolution images of heart structure and function is captured by an effective non-invasive imaging tool named CMRI.

A comprehensive insights regarding cardiovascular health is offered by CMRI via the supply of detailed assessments of blood flow, myocardial tissues, and cardiac morphology [2-4]. An automated solutions are needed for improving the accuracy and

Received: 03.02.2025 ***Accepted: 18.02.2025*** ***Published on: 30.06.2025***
****Corresponding Author: radhips8@gmail.com***

diagnostic efficiency, because manual analysis of these complex images are still challenging.

During MRI, the tissue visibility can be enhanced by the Contrast Agents (CA). Anomalies like tumors are differentiated by the support of CA. For accurate diagnosis and treatment strategies are not attained by CA alone. This will stress the demand for advanced classification methods. The computational models with Medical Imaging (MI), the diagnostic accuracy can be enhanced by the ML [5-7].

Initially, the labelled datasets of CMRI are used to train ML models like artificial neural networks (ANNs) or support vector machines (SVMs) [8].

An automated detection and classification of CVD is facilitated by these models. Thus, accelerating diagnosis, reducing interpretive errors, and improving CDM was also facilitated by these models [9-12].

To attain ED of CVD and classifying MRI, a novel ML-based method was introduced in this study.This study investigates a novel machine learning (ML) method for cardiac MRI image classification in order to detect CVD early. In order to address problems with CE and NR for improved CMRI IQ, it integrates the hybrid COA-SCSO optimisation technique based on cetacean behaviour with the SCSO algorithm. It does this by using a diverse dataset that includes anatomical features and disease classifications.

Table 1. Summary of ML based Methodologies Implemented for Cardiac DD

Author	**Approaches**	**Result**	**Merits**	**Demerits**
Regehr et al (2020) [13]	Using a U-Net based NN (Neural Network) technique, a fully automated method for segmenting the right atrial in 4-chamber long-axis MRI image sequences	After refinement, it produced 94.9% and 4.38 mm, respectively, with promising Sørensen–Dice coefficients and Hausdorff distances of 95.2% and 4.64 mm.	More accurate predictions	It can take a long time to solve a problem that requires the use of the Graph Theory algorithm. The technique may be challenging to debug as it is complex to pinpoint precise steps algorithms take to resolve issues.
Ramesh et al (2021) [14]	CMRI using ML for the Detection of Cardiac Disease	Techniques for automatically detecting abnormalities that assist doctors	To assist in the more accurate analysis and interpretation of the CMRI, it provides an estimate of the (IQ) Image Quality.	Need for substantial amounts of high-quality data for training
Chanda, & Sarkar (2020) [15]	For a more accurate disease classification, fuzzy-based edge detection and threshold-based segmentation techniques are used.	90% increases in the accuracy of CVD diagnosis and classification	An advantage of the improved method is that there is no need of applying filtering to the image.	The main disadvantage is time complexity because we need to iterate several times.
Luo et al (2018) [16]	A novel approach to automatic LV segmentation is created that integrates a new location method with a Hierarchical Extreme	For the LV segmentation, this method produced an effective and appropriate outcome.	It lowers segmentation costs and increases classification accuracy.	High HL complexity may be required for the ELM model. This could lead to unfavorable conditions and lessen ELM's resilience.

	Learning Machine (H-ELM).			
Bratt et al (2019) [17]	A NN-based ML model was created to track the borders of the aortic valve.	While manual segmentation took 3.96 ± 0.36 min/case (12.5 h for the complete dataset), segmentation time was less than 0.01 min/case (1.2 min).	With little supervision, it processes vast amounts of data.	Unfocused on a big population

Table 1 summarizes previous research and techniques for using ML in CVD detection. Chen et al. (2023) developed a model using a derivation cohort of 150 patients who underwent clinical phase contrast (PC) cardiovascular magnetic resonance (CMR). The model was validated in a prospective cohort and tested on an external cohort acquired from different CMR sites or vendors. The U-Net-CSP (Cross Stage Partial) method was used for effective CMRI segmentation by integrating the CSP module into U-Net's encoding and decoding stages, allowing for better feature reuse and minimizing overfitting [18]. During upsampling and downsampling, the module assists in capturing complex features and retaining important information. Additionally, utilising non-contrast Cine-CMR images and radiomic features, researchers created an ML technique to distinguish between myocardial infarction (MI) and viable tissues [19]. Spearman Correlation (SC) eliminated features with high correlation ($R2 > 0.80$), and feature selection (FS) was optimised using MSVM-RFE. A variety of evaluation metrics were used to examine 10 ML techniques. Nevertheless, the MSVM-RFE technique presents difficulties because of its high processing requirements when working with big datasets, which could lower efficiency.

This study introduces a hybrid COA-SCSO optimization method, combining Cetacean behavior with Sand Cat Swarm Optimization, to enhance cardiac MRI images through contrast enhancements and noise reduction. Enhanced images are then classified using a Particle Swarm Optimization-based PSO-PSVM-GE system for cardiac disease detection.

Materials and Techniques

The proposed work implements PSO-PSVM-GE on input cardiac MR images enhanced through a hybrid algorithm based on Cetaceans and Sand Cat Swarm Optimization (COA-SCSO) for cardiac disease detection (DD). Following the enhancement process, the research proposes PSO-PSVM-GE for detecting cardiac diseases from the enhanced images, as shown in Figure 1. The C and kernel parameters of PSVM-GE are determined using PSO. The research contributes to medical imaging by introducing a hybrid optimization algorithm and classification method that collectively improve cardiac MRI image quality and enhance diagnostic accuracy. For a reliable and effective MIA, this method integrates COA-SCSO, PSO, and GE-Based Classification.

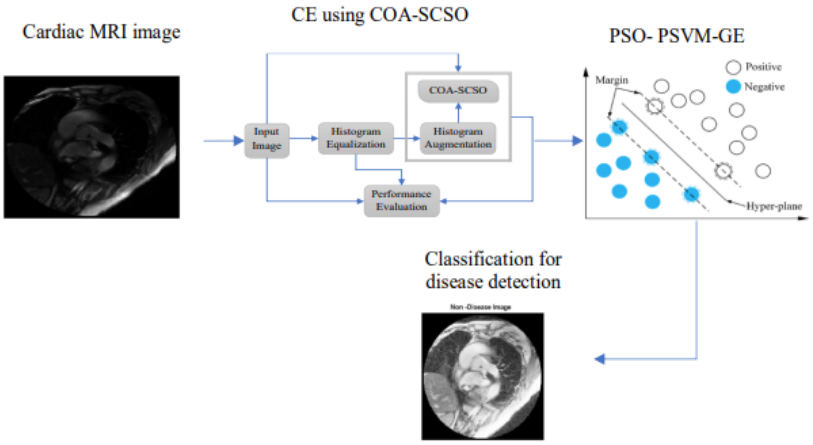

Figure 1. Architecture of Proposed Cardiac Disease Detection using PSO- PSVM-GE

CEs using COA-SCSO

Contrast enhancements (CEs) in cardiac MRI improve the visibility of structures, making it easier to distinguish various tissues or regions of interest. This section highlights how a hybrid optimization approach utilizing the Cetacean Optimization Algorithm (COA) and Sand Cat Swarm Optimization (SCSO) enhances CEs in cardiac MRI images.

1. **COA:** Inspired by the social and cooperative behaviors of cetaceans like whales and dolphins, COA is designed to solve complex optimization problems. Integrating elements from multiple algorithms further enhances its performance and efficiency.
2. **SCSO:** Modeled on the behavior of social animals like the sand cat, SCSO simulates the cooperative actions of swarms to find optimal solutions effectively.

Hybrid Optimization Process for CEs

1. **Initializations:** Set initial parameters for the hybrid optimization process, integrating COA and SCSO.
2. **Objective Functions:** Define an objective function focusing on enhancing contrast, clarity, and image quality.
3. **Repeated Enhancements:** The combined optimization method adjusts parameters iteratively, exploring the solution space by leveraging the complementary strengths of COA and SCSO.
4. **Evaluations**: Continuously assess results using visual inspections or quantitative metrics to ensure effective CEs.

By combining COA and SCSO, the proposed approach is expected to surpass the limitations of single-algorithm methods, offering more reliable and efficient contrast optimization.

Disease Detection using PSO-PSVM-GE

A novel classification algorithm is introduced, utilizing Particle Swarm Optimization (PSO), Support Vector Machine (PSVM), and Genetic Algorithm (GE) to detect cardiac diseases in enhanced MRI images.

1. **PSO:** Optimizes PSVM parameters, improving its ability to handle noisy and complex data.
2. **GE:** Assists in extracting unique and relevant features from enhanced MRI images, aiding classification accuracy.
3. **Joint strategy for disease detection:** The integration of PSO, PSVM, and GE combines parameter optimization and feature extraction, resulting in enhanced accuracy and reliability for identifying heart conditions.

Support Vector Machine (SVM)

SVM, based on the Structural Risk Minimization (SRM) paradigm, excels in

handling high-dimensional feature spaces and small sample datasets [20]. Initially developed for Pattern Recognition (PR), SVM now extends to Nonlinear Regression (NLR) problems through the introduction of the ε-insensitive loss function.

The dataset $x_i(i = 1, \dots, n)$ is converted to a (HDFS) High-Dimensional Feature Space using an NL Function (NLF) utilizing an SVM in order to solve regression issues. This is the fundamental idea behind support vector regression (SVR).

The values' relationship can be stated as equation (1),

$$f(x) = \omega^T \phi(x) + bias \quad (1)$$

Here, converting the input values into a HD space by the NL Mapping Function (MF) is denoted as $\phi(x)$, w and bias are the coefficients, and $f(x)$ is the output value. It is possible to achieve the regulated values of ω and b is represented in equation (2),

$$\begin{cases} \min R_\varepsilon(\omega^T, \phi(x), \xi) = \frac{1}{2}\omega^T\omega + C\sum_{i=1}^{n}(\xi_i^* + \xi_i), n = \\ -y_i + \omega^T\phi(x_i) + bias \le \varepsilon + \xi_i^*, \quad i = 1,2,\dots,n \\ \xi_i, \quad i = 1,2,\dots,n \end{cases} \quad (2)$$

Where $R_\varepsilon(\omega, \xi*, \xi)$: This term represents the overall risk or (OF)objective function. $\frac{1}{2}\omega^T\omega$: This part corresponds to the regularization term, where ω is the weight vector. Also represents the squared Euclidean norm of the weight vector, which is a common regularization term in SVM to control the complexity of the model. $C\sum_{i=1}^{n}(\xi_i^* + \xi_i)$): This part represents the sum of the hinge loss and the proximal term. Here, the trade-off among achieving a low training error and a low testing error is controlled by the regularization parameter C. the count of data points is denoted as n. ξ_i^* and ξ_i are the slack variables associated with the i-th data point. These variables allow for the possibility of misclassification or errors within a certain tolerance. The hinge loss is typically expressed as $\max(0, 1 - y_i(\omega^T \times x_i - bias))$, where y_i is the true label of the i-th data point, x_i is the feature vector, and $bias$ is the bias term. The hinge loss penalizes the model when a data point is on the wrong side of the decision boundary. The proximal term is usually used to make the SVM more robust to outliers. It imposes a penalty on large errors, making the model less sensitive to extreme values. The overall goal is to minimize this objective function with respect to the ω and the slack variables ξ_i^* and ξ_i. This optimization problem is typically solved using techniques such as (GD) gradient descent or specialized SVM optimization algorithms. By transforming it into a dual problem, the function above illustrates a (QOP) Quadratic Optimization Problem. The SVM's final equation (3) shown below,

$$f(x) = \sum_{i=1}^{n}(\beta_i^* - LG_i)K(x_i, x_i) + bias \quad (3)$$

Here, the inner product of two vectors is represented by the SVM kernel function $K(x_i, x_i)$, and the Lagrangian coefficients are β_i^* , LG_i. Vectors x_i and x_i kernel function is expressed below equation (4),

$$K(x_i, x_i) = \phi(x_i).\phi(x_i) \quad (4)$$

Two such kernel functions are the Gaussian kernel function and the Linear Kernel Function (LKF). The Gaussian kernel function, commonly known as the radial basis function (RBF), is one of these functions that is most widely used. Less computational effort is required to map data to an infinite dimension with this algorithm. Employ RBF for SVM, and express this function in equation (5),

$$K(x_i, x_j) = \exp\left(-\frac{\|x_i - x_j\|^2}{2\gamma^2}\right) \quad (5)$$

Where, γ is the Gaussian parameter. Outliers can cause problems for traditional SVMs. Outliers have a big effect on where the decision boundary is placed, which could result in overfitting or incorrect classifications. By introducing a proximal term, Proximal SVM becomes more robust to outliers. The proximal term penalizes large errors more heavily, helping the model resist the influence of outliers.

PSVM-GE Model

In the original SVM, two parallel planes are formed with the goal of keeping the two planes as far apart as feasible and each plane being closest to one of two datasets. In GEPSVM, the parallelism criterion on the two hyperplanes is dropped [21], and each plane must be as close to one data set as feasible and as far away from the other as feasible. According to reports, GEPSVM outperformed regular SVM in classification performance. Assume matrices $\mathbb{X}_1$ and $\mathbb{X}_2$, respectively, contain sample data from classes 1 and 2. Finding two nonparallel planes is the objective of GEPSVM in equation (6),

$$\mathcal{w}_1^T x - bias_1 = 0 \quad \text{and} \quad \mathcal{w}_2^T x - bias_2 = 0 \ (6)$$

Here the first plane is closest to class 1 points and farthest from class 2 points, while the second plane is closest to class 2 points and farthest from class 1 points. The following optimization problem results from minimizing the sum of squares of the ED among each point in class 1 and the plane divided by the squares of the ED among each point in class 2 and the plane in order to achieve the first plane in equation (7),

$$(\mathcal{w}_1, bias_1) = \arg\min \frac{\left\|\mathcal{w}^T\mathbb{X}_1 - e^T bias\right\|^2 / \|\mathbb{z}\|^2}{\|\mathcal{w}^T\mathbb{X}_2 - e^T bias\|^2 / \|\mathbb{z}\|^2} \ (7)$$

Where $\mathbb{X}_1$ and $\mathbb{X}_2$ are matrices, e is a vector, $\mathbb{z}$ is defined as the concatenation of $\mathcal{w}$ and $bias$. Simplifying equation (8) gives

$$\min_{(\mathcal{w}, bias)\neq 0} = \frac{\left\|\mathcal{w}^T\mathbb{X}_1 - e^T bias\right\|^2}{\left\|\mathcal{w}^T\mathbb{X}_2 - e^T bias\right\|^2} \ (8)$$

To lower the norm of the problem variables (w, b) used to identify the first plane in equation (9), the Tikhonov regulation term is introduced.

$$minmize\left(\frac{\|\mathbb{z}\|^2 \mathcal{w}^T\mathbb{X}_1 - e^T bias\|^2}{\|\mathbb{z}\|^2}\right) + \left(\frac{\|\mathbb{z}\|^2 \mathcal{w}^T\mathbb{X}_2 - e^T bias\|^2}{\|\mathbb{z}\|^2}\right) + \alpha(\|\ \mathcal{w}\ \|^2 + \|\ bias\ \|^2) \ (9)$$

where: α a nonnegative Tikhonov factor that is the regularization parameter that controls the strength of the regularization. The terms $\|\ \mathcal{w}\ \|^2$ and $\|\ bias\ \|^2$ are the squared norms of the weight vector $\mathcal{w}$ and the $bias$ term. Equation (10) becomes the "Rayleigh quotient" of the form

$$\mathbb{z}_1 = \arg\min \frac{\mathbb{z}^T \mathrm{G}\times\mathbb{z}}{\mathbb{z}^T \mathrm{H}\times\mathbb{z}} \ (10)$$

where G and H are symmetric matrices in $R^{(p+1)\times(p+1)}$ defined as equation (11) and (12),

$$G \stackrel{\text{def}}{=} [\mathbb{X}_1\ -e]^T[\mathbb{X}_1\ -e] + \alpha I \ (11)$$

$$H \stackrel{\text{def}}{=} [\mathbb{X}_2\ -e]^T[\mathbb{X}_2\ -e] \ (12)$$

Where, I is the identity matrix. Using the boundedness and stationarity properties of the Rayleigh Quotient, the GE problem is solved to generate an outcome of equation (11).

$$\mathrm{G}\times\mathbb{z} = \lambda\, \mathrm{H}\times\mathbb{z}\ ,\ \mathbb{z} \neq 0 \ (13)$$

Here, the smallest eigenvalue $\lambda_{\min}$min of equation (8) corresponds to an eigenvector $\mathbb{z}_1$, where the global minimum of equation (10) is reached. Therefore, equation (7) can be used to derive w_1 and b_1, which can then be used to find the plane in equation (13). The second plane, which is near points in class 2, can be obtained from the eigenvector $\mathbb{z}_2^*$, which corresponds to the smallest eigenvalue of the second GE problem. Achieving a high predicting accuracy depends critically on an accurate combination of PSVM parameters (C , ε,α and γ).

Here, γ is a parameter for the RBF kernel and C is a regularization parameter and influences the shape of the decision boundary and ε-insensitive Loss Function. The block-diagram of PSVM-GE is given in Figure 2. As a result, choose appropriate parameters using the PSO algorithm. The next subsection goes into additional detail about this algorithm.

1. Start 2. Gather and preprocess the training data, ensuring it is labeled and appropriately formatted. 3. Specify the regularization parameter for the Proximal SVM algorithm. 4. Compute the kernel matrix based on the training data. 5. Compute the Generalized Eigenvalue decomposition of the kernel matrix. 6. Calculate the optimal weights for the support vectors using the Generalized Eigenvalue regularization. 7. Apply the learned weights to classify new, unseen data points. 8. Utilizing

the proper metrics (such as accuracy, precision, and recall), assess the Proximal SVM model's performance 9. If the performance is satisfactory, proceed to step 10. Otherwise, adjust the regularization parameter or consider other modifications to improve the model. 10. End

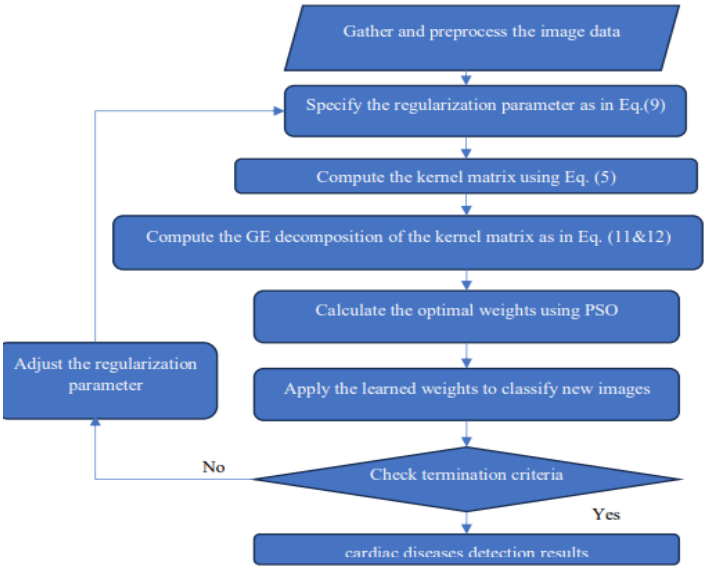

Figure 2. Flowchart of PSO-PSVM-GE for Disease Detection

Particle Swarm Optimization for Parameter Optimization of PSVM-GE

A swarm computing technique called PSO was created using iterative optimization as a foundation [22]. A group of particles is initialized by this algorithm, which then tracks two best values, the individual best value $\mathcal{P}_{ibest}$ and the global best value $\mathcal{P}_{abest}$ to adjust the particles' position and velocity in the subsequent iteration. PSO determines each particle's distance traveled and speed after determining these two extremities. Assume that a d −dimensional (SS) Search Space has a population of $,m$ particles. The representation of the $i\ -\ th$ particle is $x_i = (x_{i1}, x_{i2}, \dots, x_{id})$, $i = 1, 2, \dots, m$. Then, xi represents the location of the $i - th$ particle. $\mathbb{v}_i = (\mathbb{v}_{i1}, \mathbb{v}_{i2}, \dots, \mathbb{v}_{id})$ represents the vector, the velocity of the i-th particle.

Here, $= (\mathcal{p}_{g1}, \mathcal{p}_{g2}, \dots, \mathcal{p}_{gd})$ is the ideal position for the entire population, $\mathcal{p}_i = (\mathcal{p}_{i1}, \mathcal{p}_{i2}, \dots, \mathcal{p}_{id})$ is the optimal position for this particle. $\mathbb{v}_i$ and x_i are updated by the conventional PSO method as equation (14),

$$\mathbb{v}_{i,k+1}^{d} = \bar{w}\mathbb{v}_{i,k}^{d} + c_1 rand_1\left(\mathcal{P}_{i,k}^{d} - x_{i,k}^{d}\right) + c_2 rand_2\left(P_{g,k}^{d} - x_{i,k}^{d}\right), \quad x_{i,k+1}^{d} = x_{i,k}^{d} + \mathbb{v}_{i.k+1}^{d} \quad (14)$$

The weight coefficient of inertia is represented by $\bar{w}$, two non-negative constants known as acceleration constants are c_1, c_2, and random numbers with uniform distribution within [0,1] are denoted by $[\![rand_1, rand_2$. Premature convergence in optimization is the primary cause of PSO problems. We control the population's traits using an enhanced PSO method. When selecting the starting population, apply the following average grain spacing to avoid entering the local optimum represented in equation (15),

$$D(t) = \frac{1}{mL}\sum_{i=1}^{m}\sqrt{\sum_{d=1}^{n}\left(\mathcal{p}_i^d - \overline{\mathcal{p}^d}\right)^2}, (15)$$

Here, n indicates the solution space's size, L is the SS diagonal's maximum length, the d-dimensional coordinate value is denoted as $\mathcal{P}_i^d$. $\overline{\mathcal{p}^d}$ is the $\mathcal{P}_i^d$ mean value. Each particle's distribution dispersion degree is represented by the average particle spacing. Conversely, a higher population concentration is indicated by a smaller $D(t)$. In order to address premature convergence issues, premature convergence

judgment is essential. Since the position of a particle plays a major role in determining its fitness, the overall change in the fitness of all particles can be used to estimate the population's present condition.

Then, f_i represents the current fitness and $\bar{f}$be the current average fitness. The population's fitness variance is defined as follows equation (16),

$$\lambda^2 = \sum_{i=1}^{m} \left(\frac{f_i - \bar{f}}{f}\right)^2 \quad (16)$$

Here, the normalization scaling factor (f)that is used to restrict the λ^2 size. Computing f,

$$\lambda^2 = \sum_{i=1}^{m} \left(\frac{(f_i - \bar{f})}{f}\right)^2 \quad (17)$$

Here, the particle aggregation degree is denoted by λ^2. Greater aggregation degree is correlated with smaller λ^2, and vice versa in equation (17). Because the fitness increases and becomes closer, the value of λ^2 steadily decreases as the amount of iterations increases.

Meanwhile, the algorithm goes into the latter search step when $\lambda^2 \prec$ (where β is a predetermined threshold value). Find the best possible combination of new training data classes and input variables in the analysis above. Next, create a novel hybrid PSO–PSVM–GE model in order to acquire predicted outcomes. To find the ideal PSVM-GE settings, and employ PSO. The method of the suggested PSO-PSVM-GE model is detailed in depth in Figure 3.

Prior to determining the population size m, the acceleration constants c_1 and c_2, the maximum evolutionary algebra $T_{\max}$, or the iterative termination threshold, the particle population is initialized. Then choose m = 20, set the maximum evolutionary algebra $T_{\max} = 200$, and utilize the range [0.4,0.9] as our values. Set c_1 and c_2 to 2 at start to equalize the effects of random factors. An automatic optimization may generate the values of the SVM parameters C, ε and γ.

Creating a PSO-based Proximal SVM-GE model involves several steps. Below are the general algorithmic steps for building such a model:

1. **Initialization:** Start a particle swarm, with each particle representing a potential solution in the model's parameter space, including SVM and GE parameters. Assign initial positions and velocities to particles.
2. **Model development:** Define an objective function (OF) to assess model performance. The primary classifier is the Proximal SVM, incorporating GE-based feature extraction. The OF guides PSO toward optimization.
3. **Fitness evaluations:** Evaluate each particle's fitness by training the Proximal SVM with GE using the particle's parameter values and assessing performance on the training dataset.
4. **Updating personal best positions:** Update a particle's personal best position if its current fitness exceeds its previous best.
5. **Global best update:** Determine and update the swarm's global best position based on particles with the highest fitness.
6. **Velocities and positional adjustments:** Adjust particle positions and velocities according to PSO updates, recalibrating Proximal SVM and GE parameters using both personal and global best positions.
7. **Iteration:** Repeat steps 3 to 6 until convergence or a predefined iteration limit is reached.
8. **Optimal solution extraction:** Extract the best parameter values for the Proximal SVM-GE model identified through the PSO process.
9. **Model training:** Train the final Proximal SVM with GE using the optimized parameters obtained through PSO.

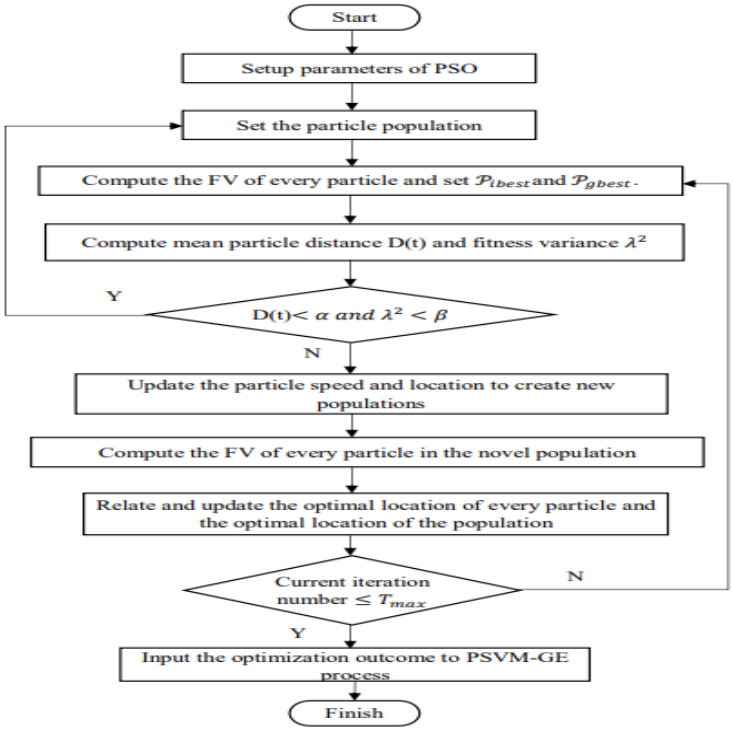

Figure 3. Flowchart of PSO-PSVM-GE

Experimental Results and Discussion

This section presents the results of the proposed framework compared to other methodologies using CMRI images from the AMRG Atlas and SCMR databases.

The AMRG Atlas and SCMR image collections serve as vital resources for cardiovascular imaging research, offering comprehensive references for researchers, clinicians, and educators. These databases include diverse MRI images depicting typical anatomical structures and various cardiovascular diseases (CVDs) and conditions. It is easier to identify specific features and abnormalities due to the meticulously labelled images. This will make it possible to compare states of health and illness. By examining how various illnesses affect the heart, main vessels, and surrounding cardiac structures, researchers might improve diagnostic and therapeutic approaches. The advancement of imaging techniques and the creation of novel ways to cardiovascular treatment are greatly aided by these datasets.

Figures 4 and 5 illustrate key results from the framework. Figure 4 displays improved output images alongside their corresponding input images representing diseased states, highlighting the effectiveness of image enhancement in identifying anomalies. Figure 5 shows augmented input images and their associated outputs reflecting non-diseased conditions, demonstrating the system's ability to differentiate healthy cardiac structures. The overall framework supports enhanced diagnostic precision and treatment planning for CVDs.

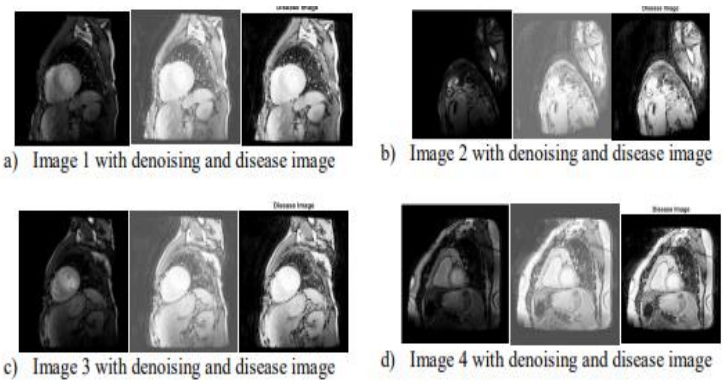

Figure 4. Comparison of Original Cardiac MRI Images with Denoising and Disease Image

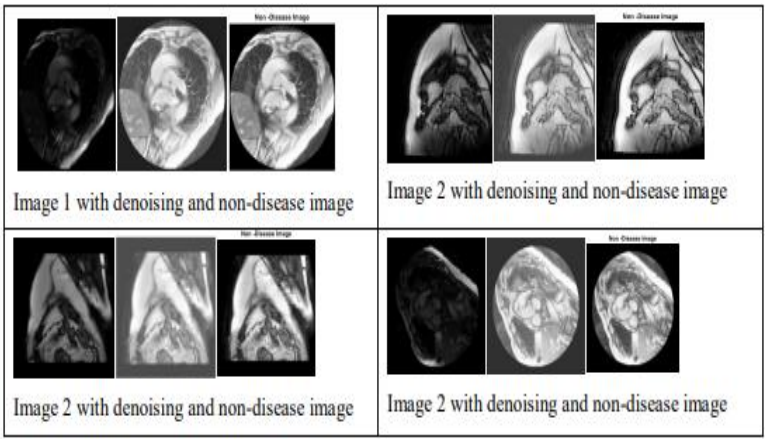

Figure 5. Comparison of Original Cardiac MRI Images with Denoising and Non-disease Image

Results Discussion

In this part, we test and compare the performance of the proposed PSO-PSVM-GE model for cardiac disease detection and classification to current fuzzy-based approaches [15], H-ELM [16], and MSVM-RFE [19]. The performance was measured in terms of accuracy in equation (18), sensitivity in equation (19), specificity in equation (20), precision in equation (20) and F1-score in equation (21).

$$Accuracy = \frac{TP+TN}{TP+TN+FP+FN} \quad (18)$$

$$Sensitivity\ (Recall) = \frac{TP}{TP+FN} \quad (19)$$

$$Specificity = \frac{TN}{TN+FP} \quad (20)$$

$$Precision = \frac{TP}{TP+FP} \quad (21)$$

$$F1-Score = \frac{2\times Precision\times Sensitivity}{Precision+Sensitivity} \quad (22)$$

Here, False Negative (FN) is the number of incorrectly predicted negative instances (predicted as not having cardiac disease, but actually positive), True Positive (TP) is the amount of correctly predicted positive instances (presence of cardiac disease), False Positive (FP) is the amount of incorrectly predicted positive instances (predicted as cardiac disease, but actually not), True Negative (TN) is the amount of correctly predicted negative instances (absence of cardiac disease).

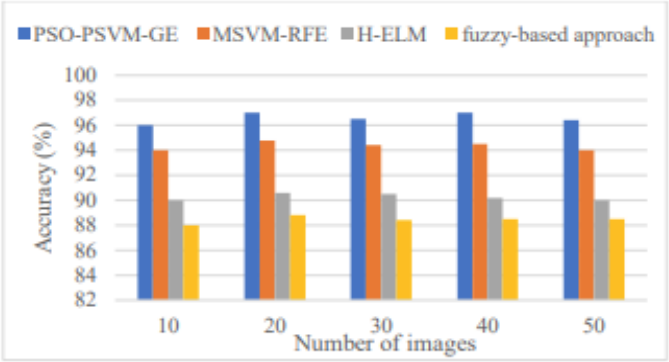

Figure 6. Comparison of Accuracy among PSO-PSVM-GE and Others

Figure 6 gives the accuracy performance comparison among proposed PSO-PSVM-GE and existing classification schemes like MSVM-RFE, H-ELM and fuzzy-based approach for the number of histological mages in a given database. As well as the accuracy is increased while reducing the computation time. The PSO-PSVM-GE attains the high accuracy of 97.5% compared existing algorithms. Cardiac MRI images often contain intricate patterns and subtle features that may be indicative of specific diseases or conditions. The PSO-PSVM-GE, allows for the identification and utilization of relevant image features that contribute to accurate disease detection [20]. The optimization process helps in finding the optimal decision boundary that separates different classes in the high-dimensional feature space, making it effective in capturing complex patterns present in cardiac MRI images. The Generalized Eigenvalue approach can enhance the discriminative power of the SVM by incorporating class-specific information, contributing to better separation of different disease classes in the image data.

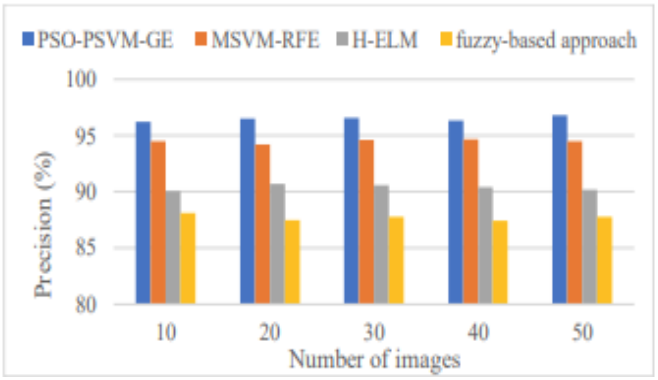

Figure 7. Comparison of Precision among PSO-PSVM-GE and Others

Figure 7 gives the precision performance comparison among proposed PSO-PSVM-GE and existing classification schemes like MSVM-RFE, H-ELM and fuzzy-based approach for the amount of histological images in a assumed database. The PSO-PSVM-GE attains the high precision of 97.3% compared existing algorithms. In the context of cardiac MRI image disease detection, a high precision rate means that the algorithm is effective in minimizing FP. FP exist when the framework inaccurately detects a healthy case as diseased. This is particularly crucial in clinical applications where misdiagnoses can lead to unnecessary interventions or stress for patients [21]. The PSO-PSVM-GE, contributes to the selection of relevant features and optimal hyperplane, resulting in a model that is more discriminative and less prone to misclassifying normal cases as diseased. In summary, the

advantage of a high precision rate is the ability of the PSO-PSVM-GE to minimize the occurrence of false positives in cardiac MRI image disease detection.

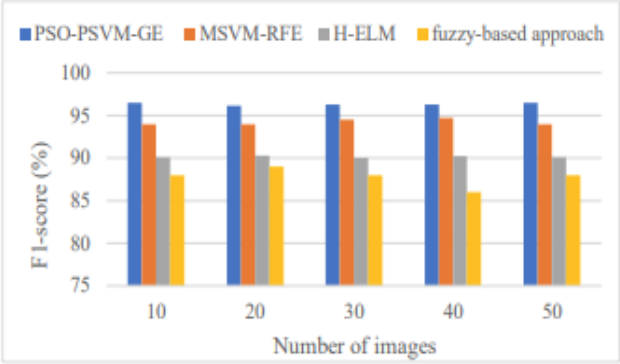

Figure 8. Comparison of F1-score among PSO-PSVM-GE and Others

Figure 8 compares the F1-score performance of the proposed PSO-PSVM-GE with existing classification methods like MSVM-RFE, H-ELM, and fuzzy-based approaches using histological images from an assumed database. The PSO-PSVM-GE achieves a high F1-score of 97.5%, surpassing other algorithms, while optimizing hybrid CFCM scheme hyperparameters with lower computational cost. This high F-measure indicates a balance between recall (sensitivity) and precision, crucial for accurate cardiac MRI disease detection [22]. Minimizing false positives (FP) prevents unnecessary interventions, while reducing false negatives (FN) avoids missed diagnoses and delayed treatment. Thus, PSO-PSVM-GE ensures both high precision and effective identification of true positives (TP), improving overall diagnostic accuracy.

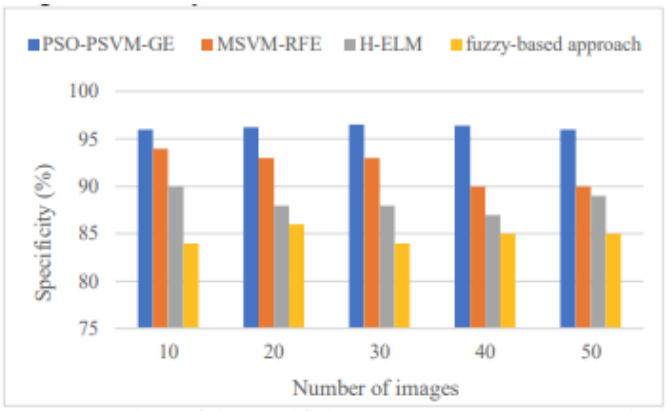

Figure 9. Comparison of the Specificity among PSO-PSVM-GE and Others

Figure 9 compares the specificity performance of PSO-PSVM-GE with existing methods like MSVM-RFE, H-ELM, and fuzzy-based approaches using histological images from an assumed database. The PSO-PSVM-GE achieves high specificity (96.34%) and reduced computation time compared to other algorithms. High specificity is vital in cardiac MRI disease detection for minimizing false positives, preventing unnecessary medical interventions, and reducing patient anxiety [23]. The PSO-based optimization, combined with Proximal SVM and Generalized Eigenvalue, enhances feature selection and decision boundaries, reducing false positives and improving specificity. PSO's robustness, less prone to local optima, ensures accurate detection and mitigates the impact of noisy or irrelevant features.

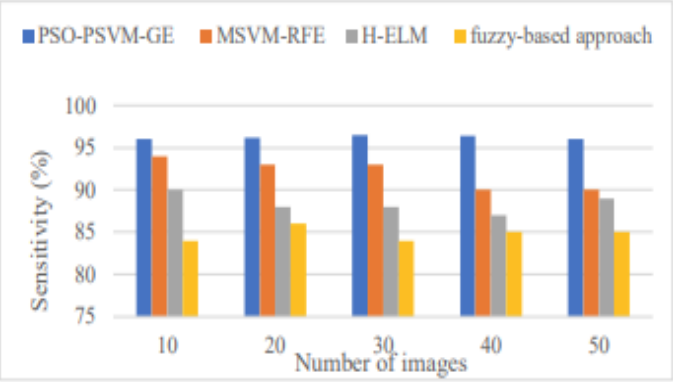

Figure 10. Comparison of Sensitivity among PSO-PSVM-GE and Others

Figure 10 compares the sensitivity performance of PSO-PSVM-GE with existing classification methods like MSVM-RFE, H-ELM, and fuzzy-based approaches using histological images from an assumed database. The PSO-PSVM-GE achieves improved sensitivity (96.8%) with reduced computation time compared to previous algorithms. Effective illness segmentation and clustering allowed the proposed CFCM and ACLAHE to outperform other systems. The PSO-PSVM-GE optimizes one layer at a time, leveraging CFCM to enhance sensitivity. Adjusting SVM parameters using PSO ensures the model performs well on new, unseen data, recognizing varying sickness patterns across patients. The PSO optimization process reduces overfitting by balancing generalizability and complexity. By efficiently searching the feature space and optimizing support vector weights in PSVM-GE, PSO enhances sensitivity by identifying key features critical for detecting cardiac MRI abnormalities.

Conclusion and Future Scope

With several benefits, the PSO-PSVM-GE approach provides a useful means of diagnosing cardiac MRI problems. PSO increases the sensitivity of MRI data-based cardiac disease detection by making it easier to modify SVM parameters. The combined global search capabilities of PSO improve feature selection, weight optimization, and data distribution flexibility. A model with high sensitivity, resistance to overfitting, and good generalization to fresh, unseen data is produced by combining PSO, Proximal SVM, and GE. PSO's automatic parameter tuning saves a substantial amount of time by speeding up the modeling process and doing away with the necessity for human changes. This strategy could prove beneficial.

1. Determine whether it might be beneficial to combine PSO with other optimization techniques or ML methods. Using hybrid techniques may improve model performance and generalization ability. Examine specifically how PSO functions with DL architectures such as CNNs and RNNs for applications including feature extraction and illness diagnosis.
2. Given DL models perform well in image processing, combining them with PSO may improve results even more. Extensive validation research utilizing sizable datasets that span a variety of patient demographics is necessary to assess the generalizability and robustness of these models. A range of MRI scanner technology and acquisition techniques must be covered in performance assessments.
3. Assess the degree to which online learning strategies adapt to changing data sources. This functionality is particularly crucial in the healthcare industry because patient demographics and imaging technologies are subject to change over time.

Acknowledgement

The authors are thankful to Manav Rachna International Institute of Research and Studies for supporting in completion of the research work.

Author Contribution

R. Radhika: Methodology, Writing – original draft, Conceptualization, Supervision

Dr. Rashima Mahajan: Data collection and analysis, Writing – review &amp, Data interpretation

Conflict of Interest

The authors declare no conflict of interest related to the publication of this manuscript.

Funding

This research received no external funding.

Ethical Approval Statement

This study did not require ethical approval as it did not involve human participants, animal subjects, or any procedures requiring such approval under prevailing guidelines.

References

[1]. Guo, R., Weingärtner, S., Šiurytė, P., Stoeck, C. T., Fütterer, M., Campbell-Washburn, A. E., Suinesiaputra, A., Jerosch-Herold, M., & Nezafat, R., 2022, Emerging techniques in cardiac magnetic resonance imaging, *Journal of Magnetic Resonance Imaging*, 55(4), 1043-1059.

[2]. Mangold, S., Kramer, U., Franzen, E., Erz, G., Bretschneider, C., Seeger, A., Claussen, C. D., Niess, A. M., & Burgstahler, C., 2013, Detection of cardiovascular disease in elite athletes using cardiac magnetic resonance imaging. RöFo-Fortschritte auf dem Gebiet der Röntgenstrahlen und der bildgebenden Verfahren, 185(12), 1167-1174.

[3]. Bi, W. L., Hosny, A., Schabath, M. B., Giger, M. L., Birkbak, N. J., Mehrtash, A., Allison, T., Arnaout, O., Abbosh, C., Dunn, I. F., & Mak, R. H., 2019, Artificial intelligence in cancer imaging: clinical challenges and applications. *CA: A Cancer Journal for Clinicians*, 69(2), 127-157.

[4]. Khairnar, S., More, N., Mounika, C., & Kapusetti, G., 2019, Advances in contrast agents for contrast-enhanced magnetic resonance imaging. *Journal of Medical Imaging and Radiation Sciences*, 50(4), 575-589.

[5]. Dey, D., Slomka, P. J., Leeson, P., Comaniciu, D., Shrestha, S., Sengupta, P. P., & Marwick, T. H., 2019, Artificial intelligence in cardiovascular imaging: JACC state-of-the-art review. *Journal of the American College of Cardiology*, 73(11), 1317-1335.

[6]. Tan, L. K., Liew, Y. M., Lim, E. Y., & Abdul Aziz, Y. F., 2019, A comprehensive review on automated diagnosis of cardiac disease using different machine learning paradigms. *Computer Methods and Programs in Biomedicine*, 182, 105055.

[7]. Giger, M. L., 2018, Machine learning in medical imaging. *Journal of the American College of Radiology*, 15(3), 512-520.

[8]. Rana, M., & Bhushan, M., 2023, Machine learning and deep learning approach for medical image analysis: diagnosis to detection. *Multimedia Tools and Applications*, 82(17), 26731-26769.

[9]. Dinesh, P., Vickram, A. S., & Kalyanasundaram, P., 2024, Medical image prediction for diagnosis of breast cancer disease comparing the machine learning algorithms: SVM, KNN, logistic regression, random forest and decision tree to measure accuracy. *AIP Conference Proceedings*, 2853(1).

[10]. Erickson, B. J., Korfiatis, P., Akkus, Z., & Kline, T. L., 2017, Machine learning for medical imaging. Radiographics, 37(2), 505-515.

[11]. Singh, P., Singh, N., Singh, K. K., & Singh, A., 2021, Diagnosing of disease using machine learning. *In* Machine learning and the internet of medical things in healthcare (pp. 89-111).

[12]. Tarroni, G., Oktay, O., Bai, W., Schuh, A., Suzuki, H., Passerat-Palmbach, J., De Marvao, A., O'Regan, D. P., Cook, S., Glocker, B., & Matthews, P. M., 2018, Learning-based quality control for

cardiac MR images. *IEEE Transactions on Medical Imaging*, 38(5), 1127-1138.

[13]. Regehr, M., Volk, A., Noga, M., & Punithakumar, K., 2020, Machine learning and graph-based approach to automatic right atrial segmentation from magnetic resonance imaging. In 2020 IEEE 17th *International Symposium on Biomedical Imaging (ISBI)* (pp. 826-829).

[14]. Ramesh, M., Mandapati, S., Prasad, B. S., & Kumar, B. S., 2021, Machine learning-based cardiac magnetic resonance imaging (CMRI) for cardiac disease detection. In 2021 Second International Conference on Smart Technologies in Computing, *Electrical and Electronics (ICSTCEE)* (pp. 1-5).

[15]. Chanda, P. B., & Sarkar, S. K., 2020, Cardiac MR images segmentation for identification of cardiac diseases using fuzzy-based approach. I*n* 2020 Third International Conference on Smart Systems and Inventive Technology (ICSSIT) (pp. 1238-1246).

[16]. Luo, Y., Yang, B., Xu, L., Hao, L., Liu, J., Yao, Y., & Vosse, F. V. D., 2018, Segmentation of the left ventricle in cardiac MRI using a hierarchical extreme learning machine model. *International Journal of Machine Learning and Cybernetics*, 9, 1741-1751.

[17]. Bratt, A., Kim, J., Pollie, M., Beecy, A. N., Tehrani, N. H., Codella, N., Perez-Johnston, R., Palumbo, M. C., Alakbarli, J., Colizza, W., & Drexler, I. R., 2019, Machine learning derived segmentation of phase velocity encoded cardiovascular magnetic resonance for fully automated aortic flow quantification. Journal of Cardiovascular Magnetic Resonance, 21(1), 1.

[18]. Chen, Y., Wang, L., Ding, B., Huang, Y., Wen, T., & Huang, J., 2023, Radiologically based automated segmentation of cardiac MRI using an improved U-Net neural algorithm. Journal of Radiation Research and Applied Sciences, 16(4), 100704.

[19]. Avard, E., Shiri, I., Hajianfar, G., Abdollahi, H., Kalantari, K. R., Houshmand, G., Kasani, K., Bitarafan-Rajabi, A., Deevband, M. R., Oveisi, M., & Zaidi, H., 2022, Non-contrast Cine Cardiac Magnetic Resonance image radiomics features and machine learning algorithms for myocardial infarction detection. *Computers in Biology and Medicine*, 141, 105145.

[20]. Pisner, D. A., & Schnyer, D. M., 2020, Support vector machine. In Machine learning (pp. 101-121).

[21]. Zhang, Y., Dong, Z., Liu, A., Wang, S., Ji, G., Zhang, Z., & Yang, J., 2015, Magnetic resonance brain image classification via stationary wavelet transform and generalized eigenvalue proximal support vector machine. *Journal of Medical Imaging and Health Informatics*, 5(7), 1395-1403.

[22]. Jain, M., Saihjpal, V., Singh, N., & Singh, S. B., 2022, An overview of variants and advancements of PSO algorithm. *Applied Sciences*, 12(17), 8392.

[23]. Jordehi, A. R., 2015, Enhanced leader PSO (ELPSO): a new PSO variant for solving global optimisation problems. *Applied Soft Computing*, 26, 401-417.